



Published in final edited form as:

Semin Ophthalmol. 2012 ; 27(0): 138–148. doi:10.3109/08820538.2012.711416.

In Vivo Confocal Microscopy in Dry Eye Disease and Related Conditions

Albert Alhatem, Bernardo Cavalcanti, and Pedram Hamrah

Ocular Surface Imaging Center, Cornea & Refractive Surgery Service, Massachusetts Eye & Ear Infirmary, Department of Ophthalmology, Harvard Medical School, Boston, MA, USA

Abstract

A new era of ocular imaging has recently begun with the advent of *in vivo* confocal microscopy (IVCM), shedding more light on the pathophysiology, diagnosis, and potential treatment strategies for dry eye disease. IVCM is a noninvasive and powerful tool that allows detection of changes in ocular surface epithelium, immune and inflammatory cells, corneal nerves, keratocytes, and meibomian gland structures on a cellular level. Ocular surface structures in dry eye-related conditions have been assessed and alterations have been quantified using IVCM. IVCM may aid in the assessment of dry eye disease prognosis and treatment, as well as lead to improved understanding of the pathophysiological mechanisms in this complex disease. Further, due to visualization of subclinical findings, IVCM may allow detection of disease at much earlier stages and allow stratification of patients for clinical trials. Finally, by providing an objective methodology to monitor treatment efficacy, image-guided therapy may allow the possibility of tailoring treatment based on cellular changes, rather than on clinical changes alone.

Keywords

Ocular surface; Meibomian gland; Nerves; Dry eye disease; *In vivo* confocal microscopy

INTRODUCTION

Dry eye syndrome (DES), with a prevalence of 10% to 20% of the adult population, is one of the most common disorders of the eye. As such, it is one of the most frequently encountered ocular diseases in the clinic. The high prevalence of DES is associated with a significant economic burden. Significant advances by both basic and clinical researchers have been made over the past years towards understanding the disease and the development of new treatment modalities. The International Dry Eye Workshop (2007) defined dry eye as a “multifactorial disease of the tears and ocular surface that results in symptoms of discomfort, visual disturbance, and tear film instability with potential damage to the ocular surface. It is accompanied by increased osmolarity of the tear film and inflammation of the

© 2012 Informa Healthcare USA, Inc.

Correspondence: Pedram Hamrah, MD, Ocular Surface Imaging Center, Massachusetts Eye & Ear Infirmary, Cornea Service, 243 Charles Street, Boston, MA 02114, USA. pedram_hamrah@meei.harvard.edu.

Declaration of interest: The authors report no conflicts of interest. The authors alone are responsible for the content and writing of the paper.

ocular surface.”¹ More recently, the International Workshop on Meibomian Gland Dysfunction (2010) defined meibomian gland dysfunction (MGD) as a “chronic, diffuse abnormality of the meibomian glands, commonly characterized by terminal duct obstruction and/or qualitative/quantitative changes in the glandular section. It may result in alteration of the tear film, symptoms of eye irritation, clinically apparent inflammation, and ocular surface disease.”² Although these definitions provide clear descriptions of the disease components, in-depth investigation of the pathophysiological mechanisms are still required, as they remain elusive. Moreover, as all clinical trials for new dry eye treatments in the United States have failed since 2002, the treatment of this condition presents a significant challenge for ophthalmologists.

Corneal *in vivo* confocal microscopy (IVCM) is a novel, noninvasive, high-resolution tool that allows imaging the living cornea at the cellular level, providing images comparable to histochemical methods. IVCM enables the study of corneal epithelial cells, keratocytes, endothelial cells, nerves, and the immune cells in different ocular and systemic diseases, many of which are not visible by slit-lamp examination. The ability of the new laser IVCM to examine the ocular surface has opened new doors for investigating the enigma of DES. Recent IVCM studies have provided additional insight into the etiology of DES and allow monitoring cellular changes in the cornea of the same patients over time.

In this review, we will summarize the *in vivo* confocal microscopic findings of the tissues targeted in dry eye syndrome, including the cornea, conjunctiva, and meibomian glands. By no means are we providing an exhaustive review of the literature, but rather summarizing key IVCM findings in DES and related conditions. Given the importance of understanding cellular changes in DES, there is an exciting emerging role for IVCM evolving not only for the diagnosis of DES, but also for stratification of patients for management and clinical trials, and potentially as a more objective tool to measure treatment efficacy.

MATERIALS AND METHODS

Articles assessed for inclusion in this review were identified by an electronic search of PubMed databases in December 2011 using individual and combinations of keywords “*in vivo*,” “confocal,” “microscopy,” “cornea,” “conjunctiva,” “meibomian,” “Sjögren’s syndrome,” “ocular surface,” and “dry eye,” as well as by review of the references section of the identified publications. Review and synthesis of the selected literature that has studied the histopathologic changes of the ocular surface and the meibomian glands under the confocal microscope was included.

RESULTS

Corneal Epithelium

The corneal epithelium, which is affected in DES, consists of three cellular epithelial layers, including the superficial epithelial cell layer, the intermediate or suprabasal epithelial cell layer, and the basal epithelial cell layer (Figure 1). The corneal epithelium provides an important barrier function against pathogens and other deleterious agents, and plays an important role in the ocular surface homeostasis. Previous IVCM studies have assessed the

cellular density of epithelial layers, and evaluated the abnormal morphological changes of the epithelium. Tuominen et al.³ initially described patchy alterations or irregularities of surface epithelial cells in Sjögren's Syndrome. Since then, additional studies have demonstrated a decrease in epithelial cell density as result of DES (Table 1).

Specifically, in a study by Benitez del Castillo et al., the density of the superficial epithelial cells was noted to differ significantly between primary Sjögren's dry eye (PSDE; 536–947 cells/mm²), non-Sjögren's dry eye (NSDE; 785–1258 cells/mm²), normal eyes in subjects less than 60 years of age ($N < 60$; 1299–1758 cells/mm²), as well as normal subjects greater 60 years of age ($N > 60$; 1312–1733 cells/mm²).⁴ In contrast, the density of the basal epithelial cells showed no statistical significance in between the PSDE group (5746–6599 cells/mm²) vs. NSDE group (5425–6044 cells/mm²); $N < 60$ group (5217–6348 cells/mm²) or $N > 60$ group, (5168–6062 cells/mm²).⁴

Erdélyi et al., using the laser IVCN, later demonstrated that superficial and intermediate epithelial cell densities in the central cornea were significantly decreased in the sicca group (702–984 and 4612–5444 cells/mm², respectively) as compared to normal participants (1026–1398 and 5437–6171 cells/mm², respectively).⁵ They further demonstrated that the epithelial thickness was significantly reduced in patients with lagophthalmos (37.9–51.3 μ m) as compared to normal controls (48.8–65.1 μ m), sicca patients (45.8–56.6 μ m), and dysthyroid patients (43.2–57.8 μ m).⁵ Moreover, Villani et al.⁶ demonstrated that patients with PSDE had a significantly decreased density in superficial cells, but increased density of basal epithelial cells with (965 ± 96 and 6261 ± 168 cells/mm²) compared to normal controls (1485.55 ± 133.74 and 5861.65 ± 260.40 cells/mm²). However, they did not find statistical significance between patients with PSDE and NSDE.⁶

More recently, Zhang et al.⁷ showed significantly decreased cell densities in the superficial, intermediate, and basal epithelial layers in mild dry eyes with (890 ± 197 , 5917 ± 1072 , 9234 ± 1365 cells/mm²), and moderate to severe dry eye with (746 ± 125 , 5216 ± 867 , 8634 ± 998 cells/mm²), in contrast to the control group with (1228 ± 248 , 6974 ± 662 , 11307 ± 1876 cells/mm²).⁷ Together, these studies demonstrate decreased epithelial cell density in patients with DES.

Corneal Stroma and Keratocytes

The use of the IVCN has demonstrated a decrease in central corneal thickness as a result of a reduction in stromal thickness in patients with Sjögren's syndrome, as reported by Tuominen et al.³ In addition, they reported abnormal keratocytes hyperreflectivity in these patients with Sjögren's syndrome. These hyperreflective keratocytes (Figure 2) have been termed "activated" keratocytes by some authors,⁸ although it remains to be shown if these cells are potentially stromal bone marrow-derived cells. The density of activated keratocytes has been shown to be significantly higher in the dry eye associated with Graves' orbitopathy (GO) patients (6.04 ± 2.93 cells/mm²) in comparison to healthy subjects (0.42 ± 0.73 cells/mm²).⁹ Indeed, this was the only sign found to be significantly different when GO patients were compared to control subjects, and when active GO was compared to inactive GO.⁹

Benitez del Castillo et al. showed that the density of the anterior stromal cells was increased in the PSDE group (1200–1497 cells/mm²) compared to NSDE (988–1379 cells/mm²), N < 60 (965–1248 cells/mm²), and N > 60 groups (931–1219 cells/mm²), with no statistically significant difference between the groups, however. The density of the posterior stromal cells was increased in the PSDE group, (729–887 cells/mm²) versus NSDE group (687–903 cells/mm²); and N < 60 group (645–837 cells/mm²) versus N > 60 group (682–854 cells/mm²), with no statistically significant difference between the studied groups.⁴

Corneal Nerves

Sub-basal nerve density declines linearly by 0.9% per year according to Niederer et al.¹⁰ However, studies present conflicting results regarding the effect of dry eye on sub-basal nerve density (Table 2). A significant reduction in sub-basal nerve density (Figure 2) has been reported in both Sjögren's syndrome with $511 \pm 106 \mu\text{m}/\text{mm}^2$ and non-Sjögren's syndrome dry eye with $591 \pm 90 \mu\text{m}/\text{mm}^2$, compared to controls less than 60 years with $787 \pm 105 \mu\text{m}/\text{mm}^2$, and more than 60 years with $620 \pm 92 \mu\text{m}/\text{mm}^2$.^{26,11} Reductions in sub-basal nerves have also been noted in many other dry eye-related conditions, such as after PRK, LASIK, diabetes and infectious keratitis, such as herpes simplex keratitis, bacterial, fungal and *Acanthamoeba* keratitis.^{16,27,29,30,32,33,34}

In contrast, Ho et al.¹³ and Tuominen et al.³ observed no difference in sub-basal nerve density in dry eye patient with 5.4 ± 1.8 long nerve fiber bundles per microscopic field compared with 5.0 ± 1.4 in controls. Moreover, Zhang et al. demonstrated increased corneal nerve density in dry eye patients with Sjögren's syndrome with $1745.4 \pm 414.7 \mu\text{m}/\text{mm}^2$ and non-Sjögren's syndrome with $1423.5 \pm 609.5 \mu\text{m}/\text{mm}^2$, compared to controls with $1315.7 \pm 664.7 \mu\text{m}/\text{mm}^2$.¹⁴ These variable results may be attributed to different stages and severity of dry eye in patients enrolled in these studies.¹⁵ However, the reports agree in that increased tortuosity (grades 1–4) and reflectivity (grades 1–4) of the sub-basal nerve plexus is observed in Sjögren's syndrome with 2.62 ± 0.94 and 2.08 ± 0.78 , compared to controls with 1.20 ± 0.70 and 1.85 ± 0.87 , respectively.⁶ An increased number of bead like formations have been reported as well in Sjögren's syndrome with $364 \pm 64/\text{mm}$ and in non-Sjögren's syndrome with $307 \pm 73/\text{mm}$, compared to controls less than 60 years with $192 \pm 61/\text{mm}$, and more than 60 years with $197 \pm 50/\text{mm}$. These bead like formations either reflect nerve damage⁶ or alternatively reflect the increased metabolic activity of nerve fibers, which attempt to improve the abnormal epithelial trophism.^{3,4,6} Overall, IVCN studies in dry eye patients demonstrate a role of corneal nerve density and morphology, as well as function, in the pathogenesis of this disease.

Corneal Immune and Inflammatory Cells

Langerhans cells (LCs) are epithelial dendritic cell (DCs), which are the professional antigen presenting cells of the cornea. As such, they are an important component of the defense force by limiting inflammation by inducing tolerance or by activating T lymphocytes and recruiting other immune and inflammatory cells to the cornea to fight pathogens. The distribution of dendritiform epithelial DCs in healthy subjects decreases from the periphery towards to corneal center (Figure 2). Epithelial DCs are generally located in the proximity of the sub-basal nerve plexus.^{16,17}

Only a single study has assessed the density and distribution of DCs and other immune and inflammatory cells by IVCN in DES. In dry eye-related conditions, epithelial DC density was dramatically increased throughout the cornea (Table 3; Figure 2). Lin et al. demonstrated that DCs were significantly increased in the corneal center in non-Sjögren's syndrome dry eye (NSS) (89.8 ± 10.8 cells/mm²) and Sjögren's syndrome (SS) (127.9 ± 23.7 cells/mm²) as compared to normal subjects (34.9 ± 5.7 cells/mm²).¹⁷ In addition, they demonstrated a modest increase in DC density in the peripheral cornea of SS patients (157.2 ± 29.7 cells/mm²), whereas only a slight increase was noted in the NSS group (106.9 ± 10.5 cells/mm²), compared to normal controls (90.7 ± 8.2 cells/mm²).¹⁷ Further, they showed putative activation of epithelial DCs in dry eye patients as documented by the increased presence of dendrites. While normal corneas showed a higher frequency of DCs with dendrites in the periphery, patients with DES showed increased density of "activated" DCs in the center more than in the periphery with 3.2 ± 0.5 cells/mm² in the central cornea of controls, 9.9 ± 1.7 cells/mm² in the center of NSS patients, and 46.1 ± 17.3 cells/mm² "activated" DCs in the central cornea of SS patients.¹⁷ This increase in DC density is rather modest when compared to patients with infectious keratitis, who demonstrate an up to 20-fold increase in DC density as compared to normal subjects.¹⁶

Non-dendritic corneal epithelial leukocytes are sparse in healthy subjects (center, 1.6 ± 0.6 cells/mm²; periphery, 4.3 ± 1.3 cells/mm²). In contrast, patients with SS demonstrated dramatically increased non-dendritic leukocytes in both the center (49.0 ± 12.9 cells/mm²) and periphery (84.2 ± 36.8 cells/mm²). However, patients with NSS showed slightly increased leukocyte density centrally (4.6 ± 1.0 cells/mm²), but not peripherally (8.4 ± 3.1 cells/mm²).¹⁷

The above studies demonstrate that the density of epithelial DCs and other inflammatory cells increases in the central and peripheral cornea in patients with SS, NSS, and infectious keratitis, with significant differences between SS and NSS patients. Although morphological changes of DCs are observed, the relevance of these observations remains to be shown.

Meibomian Glands

Morphologic changes have been noticed by IVCN (Figure 3) in all meibomian gland structures in dry eye conditions (Table 4). Villani et al. demonstrated that patients with SS and MGD demonstrated increased acinar dilatation with 70 ± 42 μ m in secondary SS (SSII) and (106 ± 41 μ m) in MGD compared to primary SS (SSI) and controls with (53 ± 31 and 53 ± 14 μ m, respectively). In addition, they showed a higher reflectivity (grades 1–4) of meibum in SSI (1.7 ± 0.6), SSII (2.2 ± 0.8), MGD (3.3 ± 0.7) compared to controls (1.1 ± 0.7), and decreased diameters of meibomian gland orifices in SSI and SSII with (27.8 ± 5.9 and 20.6 ± 5 μ m, respectively) compared to controls with (34.7 ± 4.3 μ m), except for an increase it in MGD with (50 ± 9.1 μ m). The inhomogeneous appearance of the acinar wall was significantly increased in all pathologic dry eye groups, with no differences between SS and MGD patients.¹⁸ Moreover, they showed decreased acinar density in patients with MGD and SSII patients with (57 ± 21 and 97 ± 43 unit/mm², respectively), and increased acinar density in SSI with 138 ± 69 unit/mm² compared to controls with 110 ± 31 unit/mm², as well as in contact lens wearers with 129 ± 48 unit/mm² compared to controls with 119 ± 22

unit/mm².^{18,19} Meibomian gland orifice diameter and meibum reflectivity (grade 1–4) were increased in both contact lens wearers with $36 \pm 8 \mu\text{m}$ and 44 ± 16 , respectively, and MGD patients with $50 \pm 9.1 \mu\text{m}$ and 3.3 ± 0.7 , respectively, compared to controls with $45 \pm 9 \mu\text{m}$ and 33 ± 7 , respectively. However, while orifice diameter decreased in SSI ($27.8 \pm 5.9 \mu\text{m}$) and SSII ($20.6 \pm 5.1 \mu\text{m}$) compared to controls ($34.7 \pm 4.3 \mu\text{m}$), meibum reflectivity increased in SSI and SSII compared to controls (1.7 ± 0.6 , 2.2 ± 0.8 , 1.1 ± 0.7 , respectively).^{18,19} Furthermore, periglandular inflammation, basal epithelial density as well as epithelial hyperkeratinization was reported in several studies.^{18,20,21} MGD showed higher inhomogeneous appearance of the periglandular interstices and the acinar wall enlargement of glandular acinar units due to inspissation of meibum secretion and glandular atrophy with periglandular fibrosis, hyperkeratinization of ductal epithelium, infiltration and enlargement of glandular acinar units and extensive periglandular inflammatory cell with (1026.1 ± 537.3 cells/mm²) compared to controls with (56.6 ± 32.1 cells/mm²).^{20,21} Among many of the previous parameters, which have been used by many authors to diagnose MGD, inflammatory cells quantification is a potential valid key to monitor MGD treatment course.³⁶ Table 4 summarizes changes in meibomian gland structures as observed by IVCN.

Conjunctiva

Several recent reports studied the conjunctiva in dry eye patients by IVCN (Table 5).^{22–24} Hong et al.²² demonstrated conjunctival epithelial cysts formation, and decreased density of conjunctival epithelial cells and goblet cells (GC). Goblet cells were characterized by IVCN as large hyperreflective oval-shaped cells with relatively homogeneous brightness. GC density was assessed by IVCN (332 ± 137 cells/mm²) and compared to impression cytology (200 ± 141 cells/mm²) in patients with SS dry eye.²² Goblet cell density by IVCN showed significantly positive correlation with impression cytology results. Although GC density measured by IVCN was higher than by impression cytology, there was no statistically significant difference.

Villani et al. more recently demonstrated higher conjunctival epithelial cells density and lower presumed GC density in young subjects.²³ However, they did not show any effect of age on presumed conjunctival inflammatory cells. Further, they showed that patients with SS had significantly increased densities of presumed epithelial cells, GC, and inflammatory cells as compared to controls, without significant correlations among the three different cell types.²³ However, there was significant variability between the two observers. In contrast, Wakamatsu et al. recently demonstrated that patients with SS had decreased conjunctival epithelial cell densities compared to healthy control subjects.²⁴ They also showed decreased conjunctival epithelial cell density in the patients with NSS dry eye. Furthermore, while SS patients showed a significant increase in conjunctival epithelial microcyst density compared to healthy control, NSS dry eye patients did not report a significant change to microcyst density. Finally, the mean conjunctival inflammatory cell density was significantly higher in the SS eyes (433 ± 435.8 cells/mm²), and NSS eyes (134.8 ± 124.2 cells/mm²), in contrast to healthy control eyes (10 ± 17.9 cells/mm²).²⁴ Thus, IVCN is beginning to provide an insight into cellular changes in the conjunctiva in patients with DES, demonstrating decreased GC density and increased inflammatory cell density.

DISCUSSION

The recent development of *in vivo* confocal microscopy has allowed the real-time investigation of cell morphology *in situ* and the evaluation of various cell populations on the ocular surface at microscopic resolution. This optical sectioning allows visualization and analysis of epithelial cells, stromal keratocytes, corneal nerves, endothelial cells, goblet cells, meibomian glands, as well as immune and inflammatory cells that previously could not be seen by slit-lamp examination. Thus, it may not only be used for diagnostic purposes, but may also provide a valuable tool in monitoring disease and measuring therapeutic efficacy in patients with dry eye syndrome.

In vivo confocal microscopic observations of the corneal epithelium in dry eye patients demonstrates significant alterations in the corneal epithelium, presumably due to increased desquamation of the superficial cell layer and inflammatory mediators.²⁵ The damage to corneal epithelium may be related to the hyperosmolarity of the tear film associated with increased tear evaporation, which may in result in the morphological and proinflammatory changes to the corneal epithelium, as well as the disruption of the ocular surface homeostasis.⁷ Increased levels of tumor necrosis factor (TNF)- α and interleukin (IL)-I could potentially result in epithelial cell apoptosis, as well as in an increased proteolytic activity at the stromal level.²⁶

In the stroma, Efron et al.⁸ described the activation of corneal keratocytes in dry eye related conditions. Further, Tuominen et al.³ observed abnormal stromal hyperreflectivity in SS. While keratocyte nuclei can be identified as discrete hyperreflective structures in the stroma, their cytoplasm, cell wall, and processes may be visible, particularly in the posterior stroma. Although anterior stromal keratocytes density decreases throughout life, the IVCN results in dry eye patients are not conclusive. Moreover, it should be noted that currently no clear guidelines exist to differentiate keratocytes from resident or migratory stromal bone marrow-derived cells, and that the differences noted in keratocyte density could be due to the level of stromal immune and inflammatory cells that were not differentiated from keratocytes.

Recently, IVCN has allowed real-time studies on corneal nerves, which has been of great interest to clinicians and scientists.^{11–16, 28} IVCN has demonstrated dramatic changes in the sub-basal nerve layer in dry eye related conditions. Sub-basal and stromal nerves undergo significant decrease in the number and the density. Further, IVCN demonstrates the abnormal morphology of sub-basal nerves, as seen by the increase in bead-like formation, sprouts, tortuosity, irregular branching patterns, and neuromas, which may be explained by nerve degeneration and regeneration, leading to active neural growth.³ The beading observed in patients with DES may be characteristic of metabolically active of transmitter-containing nerve fibers or alternatively a sign of inflammation-induced nerve damage. Neuropeptides may be involved in regeneration of corneal nerves and studies assessing neuropeptide levels may shed light into the pathophysiological mechanism of corneal nerve changes observed (e.g. nerve sprouting).

More recently, the non-invasive assessment of immune and inflammatory changes has become possible by laser IVCN that now allows visualization of these cell components not visible with previous white light IVCN machines. This is of particular interest in patients with DES, as over the past decade the role of inflammation in dry eye disease has become apparent. The increased density of epithelial DCs observed by Lin et al. may indicate a heightened immune status of the cornea.¹⁷ Thus, dynamic *in vivo* assessment of the central corneal inflammatory cell density may serve as an indicator of dry eye severity and provide new insight for dry eye treatment. As insights into the inflammatory status of the cornea that cannot be easily determined by slit-lamp examination, IVCN will not only be of help in evaluating dry eye severity, but likely guide clinical treatment, and aid in the evaluation of the efficacy of anti-inflammatory drugs in clinical trials.

IVCN has recently been applied for the examination of meibomian glands, providing a new tool to assess morphologic changes. This approach demonstrated diagnostic value of acinar density and diameter in the diagnosis of MGD.²¹ According to the International Workshop on Meibomian Gland Dysfunction (2010), MGD is caused primarily by terminal duct obstruction through keratinization. The MG obstruction may then lead to intraglandular cystic dilatation, meibocyte atrophy, gland dropout, and low secretion, effects that do not typically involve inflammation. The outcome of MGD is a reduced availability of meibum to the lid margin and tear film. The consequence of insufficient lipids may be increased evaporation, hyperosmolarity and instability of the tear film, increased bacterial growth on the lid margin, evaporative dry eye, and ocular surface inflammation and damage. However, IVCN images disclosed morphologic alterations in patients with MGD, including extensive periglandular inflammatory cell infiltration,²¹ the clinical significance of which remains to be determined.

Finally, in evaluating the conjunctival epithelium, minimally invasive techniques are most desirable. Although corneal morphologic alterations have been extensively studied by IVCN in SS, very few studies have investigated conjunctival alterations in DES. Clearly, the evaluation of the conjunctiva is feasible and the studies of the conjunctiva by IVCN are just in the infancy. In conclusion, IVCN is a non-invasive tool that could not only provide valuable diagnostic information in the clinic for patients with DES, but may also provide a powerful platform to assess therapeutic response in patients with dry eye syndrome as well as allow stratification of patients for clinical trials. IVCN could thus provide additional objective parameters and endpoints for clinical trials in dry eye disease.

REFERENCES

1. International Dry Eye WorkShop. The definition and classification of dry eye disease: Report of the definition and classification subcommittee of the international dry eye workshop (2007). *Ocul Surf.* 2007; 5:75–92. [PubMed: 17508116]
2. Nichols KK, Foulks GN, Bron AJ, Glasgow BJ, Dogru M, Tsubota K, Lemp MA, Sullivan DA. The international workshop on meibomian gland dysfunction-executive summary. *Invest Ophthalmol Vis Sci.* 2011; 50(5):1922–1929. [PubMed: 21450913]
3. Tuominen IS, Kontinen YT, Vesaluoma MH, Moilanen JA, Helintö M, Tervo TM. Corneal innervation and morphology in primary Sjögren's syndrome. *Invest Ophthalmol Vis Sci.* 2003; 44:2545–2549. [PubMed: 12766055]

4. Benítez del Castillo JM, Wasfy MA, Fernandez C, Garcia-Sanchez J. An *in vivo* confocal masked study on corneal epithelium and subbasal nerves in patients with dry eye. *Invest Ophthalmol Vis Sci.* 2004; 45:3030–3035. [PubMed: 15326117]
5. Erdélyi B, Kraak R, Zhivov A, Guthoff R, Németh J. *In vivo* confocal laser scanning microscopy of the cornea in dry eye. *Graefes Arch Clin Exp Ophthalmol.* 2007; 245:39–44. [PubMed: 16874525]
6. Villani E, Galimberti D, Viola F, Mapelli C, Ratiglia R. The cornea in Sjögren's syndrome: An *in vivo* confocal study. *Invest Ophthalmol Vis Sci.* 2007; 48:2017–2022. [PubMed: 17460255]
7. Zhang X, Chen Q, Chen W, Cui L, Ma H, Lu F. Tear dynamics and corneal confocal microscopy of subjects with mild self-reported office dry eye. *Ophthalmology.* 2011; 118:902–907. [PubMed: 21146227]
8. Efron N. Contact lens-induced changes in the anterior eye as observed *in vivo* with the confocal microscope. *Prog Retin Eye Res.* 2007; 26:398–436. [PubMed: 17498998]
9. Villani E, Viola F, Sala R, Salvi M, Mapelli C, Currò N, Vannucchi G, Beck-Peccoz P, Ratiglia R. Corneal involvement in Graves' orbitopathy: An *in vivo* confocal study. *Invest Ophthalmol Vis Sci.* 2010; 51:4574–4578. [PubMed: 20435595]
10. Niederer RL, Perumal D, Sherwin T, McGhee CN. Age-related differences in the normal human cornea: A laser scanning *in vivo* confocal microscopy study. *Br J Ophthalmol.* 2007; 91:1165–1169. [PubMed: 17389741]
11. Benítezdel Castillo JM, Acosta MC, Wassfi MA, et al. Relation between corneal innervation with confocal microscopy and corneal sensitivity with noncontact esthesiometry in patients with dry eye. *Invest Ophthalmol Vis Sci.* 2007; 48:173–181. [PubMed: 17197530]
12. Tuisku IS, Konttinen YT, Konttinen LM, Tervo TM. Alterations in corneal sensitivity and nerve morphology in patients with primary Sjögren's syndrome. *Exp Eye Res.* 2008; 86:879–885. [PubMed: 18436208]
13. Ho al BM, Ornek N, Zilelio lu G, Elhan AH. Morphology of corneal nerves and corneal sensation in dry eye: A preliminary study. *Eye.* 2005; 19:1276–1279. [PubMed: 15550934]
14. Zhang M, Chen J, Luo L, Xiao Q, Sun M, Liu Z. Altered corneal nerves in aqueous tear deficiency viewed by *in vivo* confocal microscopy. *Cornea.* 2005; 24:818–824. [PubMed: 16160498]
15. Cruzat A, Pavan-Langston D, Hamrah P. *In vivo* confocal microscopy of corneal nerves—analysis and clinical correlation. *Semin Ophthalmol.* 2010; 25:171–177. [PubMed: 21090996]
16. Cruzat A, Witkin D, Baniyadi N, Zheng L, Ciolino JB, Jurkunas UV, Chodosh J, Pavan-Langston D, Dana R, Hamrah P. Inflammation and the nervous system: The connection in the cornea in patients with infectious keratitis. *Invest Ophthalmol Vis Sci.* 2011; 52:5136–5143. [PubMed: 21460259]
17. Lin H, Li W, Dong N, Chen W, Liu J, Chen L, Yuan H, Geng Z, Liu Z. Changes in corneal epithelial layer inflammatory cells in aqueous tear-deficient dry eye. *Invest Ophthalmol Vis Sci.* 2010; 51:122–128. [PubMed: 19628746]
18. Villani E, Beretta S, De Capitani M, Galimberti D, Viola F, Ratiglia R. *In vivo* confocal microscopy of meibomian glands in Sjögren's syndrome. *Invest Ophthalmol Vis Sci.* 2011; 52:933–939. [PubMed: 21169534]
19. Villani E, Ceresara G, Beretta S, Magnani F, Viola F, Ratiglia R. *In vivo* confocal microscopy of meibomian glands in contact lens. *Invest Ophthalmol Vis Sci.* 2011; 52:5215–5219. [PubMed: 21571676]
20. Matsumoto Y, Sato EA, Ibrahim OM, Dogru M, Tsubota K. The application of *in vivo* laser confocal microscopy to the diagnosis and evaluation of meibomian gland dysfunction. *Mol Vis.* 2008; 14:1263–1271. [PubMed: 18618006]
21. Ibrahim OM, Matsumoto Y, Dogru M, Adan ES, Wakamatsu TH, Goto T, Negishi K, Tsubota K. The efficacy, sensitivity, and specificity of *in vivo* laser confocal microscopy in the diagnosis of meibomian gland dysfunction. *Ophthalmology.* 2010; 117:665–672. [PubMed: 20189653]
22. Hong J, Zhu W, Zhuang H, Xu J, Sun X, Le Q, Li G, Wang Y. *In vivo* confocal microscopy of conjunctival goblet cells in patients with Sjögren's syndrome dry eye. *Br J Ophthalmol.* 2010; 94:1454–1458. [PubMed: 19955202]

23. Villani E, Beretta S, Galimberti D, Viola F, Ratiglia R. *In vivo* confocal microscopy of conjunctival roundish bright objects: Young, older, and Sjögren subjects. *Invest Ophthalmol Vis Sci.* 2011; 52:4829–4832. [PubMed: 21508113]
24. Wakamatsu TH, Sato EA, Matsumoto Y, Ibrahim OM, Dogru M, Kaido M, Ishida R, Tsubota K. Conjunctival *in vivo* confocal scanning laser microscopy in patients with Sjögren's Syndrome. *Invest Ophthalmol Vis Sci.* 2010; 51:144–150. [PubMed: 19696170]
25. Pflugfelder SC, Solomon A, Stern ME. The diagnosis and management of dry eye: A twenty-five-year review. *Cornea.* 2000; 19:644–649. [PubMed: 11009316]
26. Villani E, Galimberti D, Viola F, Mapelli C, Del Papa N, Ratiglia R. Corneal involvement in rheumatoid Arthritis: An *in vivo* confocal study. *Invest Ophthalmol Vis Sci.* 2008; 49:560–564. [PubMed: 18234999]
27. Hamrah P, Cruzat A, Dastjerdi MH, Zheng L, Shahatit BM, Bayhan HA, Dana R, Pavan-Langston D. Corneal sensation and subbasal nerve alterations in patients with herpes simplex keratitis: An *in vivo* confocal microscopy study. *Ophthalmology.* 2010 Oct.117:1930–1936. [PubMed: 20810171]
28. Darwish T, Brahma A, Efron N, O'Donnell C. Subbasal nerve regeneration after penetrating keratoplasty. *Cornea.* 2007 Sep.26:935–940. [PubMed: 17721291]
29. Erie JC, McLaren JW, Hodge DO, Bourne WM. Recovery of corneal subbasal nerve density after PRK and LASIK. *Am J Ophthalmol.* 2005; 140:1059–1064. [PubMed: 16376651]
30. Calvillo MP, McLaren JW, Hodge DO, Bourne WM. Corneal reinnervation after LASIK: Prospective 3-year longitudinal study. *Invest Ophthalmol Vis Sci.* 2004; 45:3991–3996. [PubMed: 15505047]
31. Darwish T, Brahma A, O'Donnell C, Efron N. Subbasal nerve fiber regeneration after LASIK and LASEK assessed by noncontact esthesiometry and *in vivo* confocal microscopy: Prospective study. *J Cataract Refract Surg.* 2007; 33:1515–1521. [PubMed: 17720064]
32. Kallinikos P, Berhanu M, O'Donnell C, Boulton AJ, Efron N, Malik RA. Corneal nerve tortuosity in diabetic patients with neuropathy. *Invest Ophthalmol Vis Sci.* 2004; 45:418–422. [PubMed: 14744880]
33. Malik RA, Kallinikos P, Abbott CA, et al. Corneal confocal microscopy: A non-invasive surrogate of nerve fibre damage and repair in diabetic patients. *Diabetologia.* 2003; 46:683–688. [PubMed: 12739016]
34. Rosenberg ME, Tervo TM, Immonen IJ, Muller LJ, Grönhagen-Riska C, Vesaluoma MH. Corneal structure and sensitivity in type 1 diabetes mellitus. *Invest Ophthalmol Vis Sci.* 2000; 41:2915–2921. [PubMed: 10967045]
35. Oliveira-Soto L, Efron N. Morphology of corneal nerves using confocal microscopy. *Cornea.* 2001; 20:374–384. [PubMed: 11333324]
36. Matsumoto Y, Shigeno Y, Adan Sato E, Ibrahim O, Saiki M, Negishi K, Ogawa Y, Dogru M, Tsubota K. The evaluation of the treatment response in obstructive meibomian gland disease by *in vivo* laser confocal microscopy. *Graefes Arch Clin Exp Ophthalmol.* 2009; 247(6):821–829. [PubMed: 19101718]

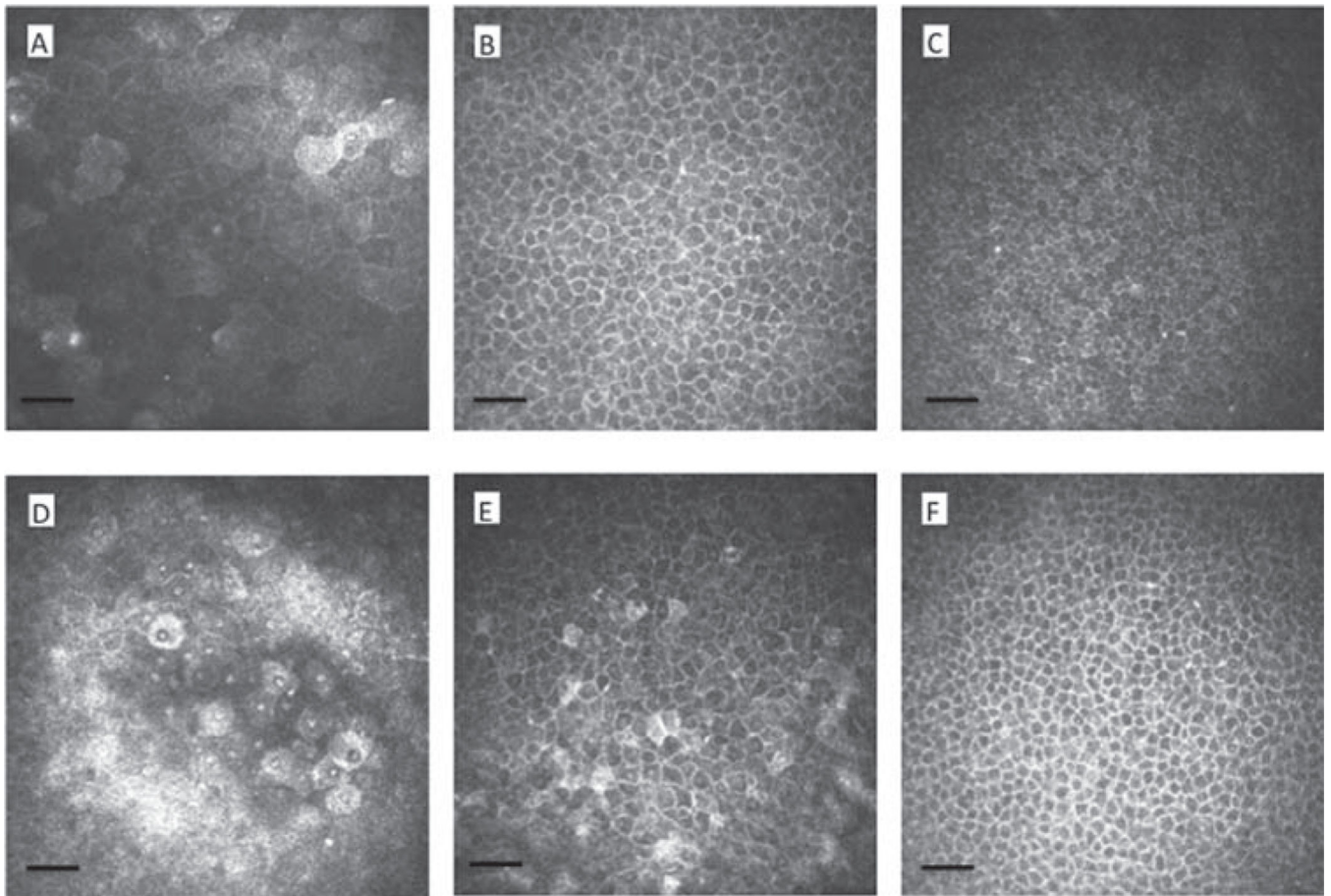


FIGURE 1.

Cornea epithelial layer in normal and dry eye patients. Normal subjects: **(A)** normal superficial epithelium with few hyperreflective cells (squamous metaplasia) and dark nuclei; **(B)** intermediate wing layer with symmetrical shape, bright cell borders and dark cytoplasm; **(C)** regularly arranged small cells with bright borders and non-homogenous cytoplasmic reflectivity. Dry eye patients: **(D–F)** epithelial squamous metaplasia (hyperreflectivity) with increase in desquamation, enlarged cells, pyknic nuclei, and lower cell density as compared to normal.

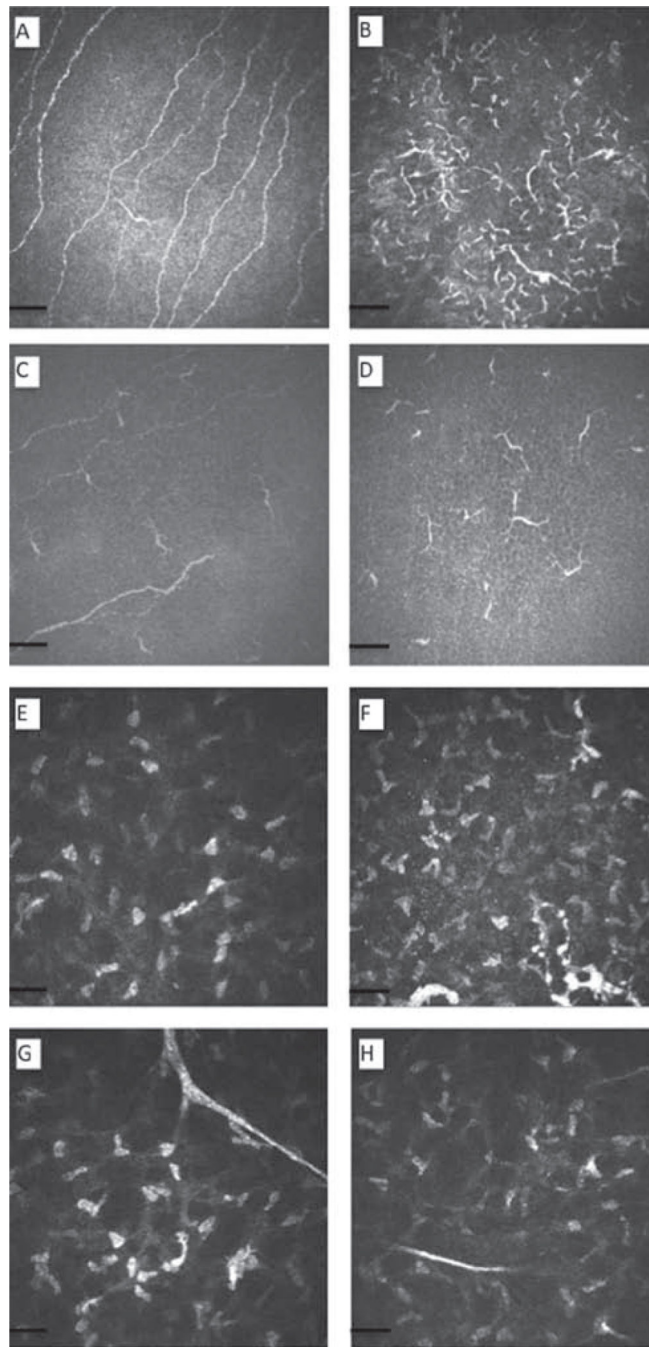


FIGURE 2.

In vivo confocal images of cornea sub-basal nerve plexus, dendritic cells, and stromal keratocytes. (A) Central and (C) peripheral sub-basal nerve plexus demonstrating normal pattern with few dendritiform cell; (B) central and (D) periphery images showing loss of nerves and increase in dendritiform cell density in dry eye patients. Stroma (E) with bright oval keratocyte nuclei and (G) stromal nerves; (F) and (H) dry eye subjects with keratocyte pleomorphism (potentially immune cells), more tortuous nerves, and decreased nerve density.

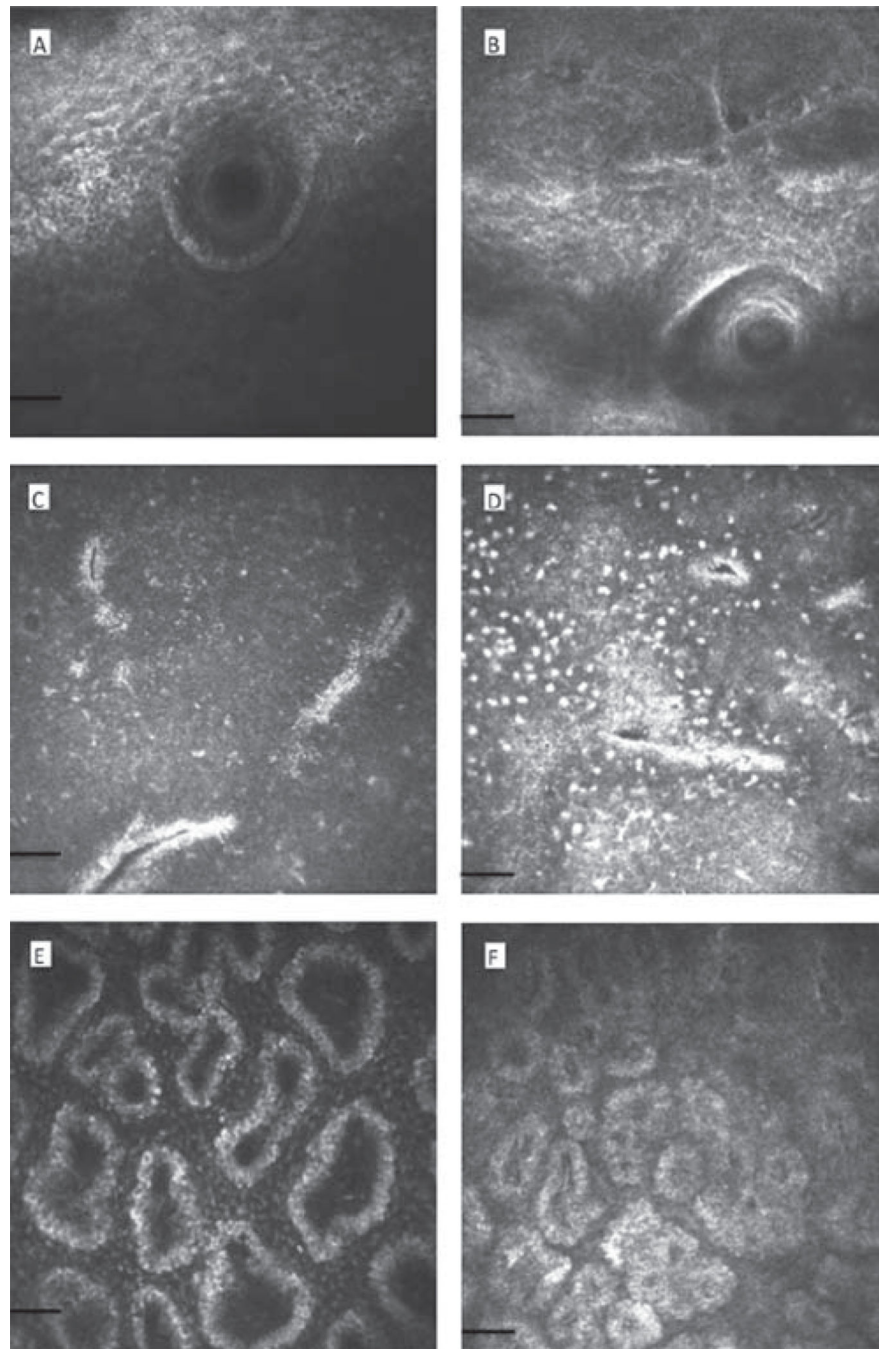


FIGURE 3.

In vivo confocal images of the lid and meibomian glands. (A) Meibomian gland orifice in normal patient and (B) closed orifice in a patient with meibomian gland dysfunction (MGD). Tarsal conjunctiva of normal subject (C). Conjunctiva shows increase in inflammatory cells in MGD patient (D) as compared to normal subject (C). Acinar meibomian gland units (E) with few hyperreflectivity areas; MGD patient with decreased acinar density, atrophic morphology, and increase in hyperreflective areas (F).

TABLE 1

Corneal epithelial and stromal changes by IVCN in dry eye-related conditions.

IVCN epithelial and stromal changes in dry eye vs. normal controls					
Study /Machine	Dry Eye conditions, Patient No.	Superficial Epithelial Cell density (cells/mm ²)	Basal Epithelial Cell Density (cells/mm ²)	Corneal Thickness (μm)	Morphology
Tuominen et al. (2003) ³ /TSCM	(SS, n = 10) (NL, n = 10)		No difference	↓ (515.9 ± 22.0 μm) [*] (547.4 ± 42.0 μm)	– Irregularities in surface epithelial cells. – Hyper-reflectivity of anterior keratocytes. – ↓Epithelial thickness
Benitez del Castillo et al. (2004) ⁴ /Confoscan-4	(SSI, n = 11) (NSS, n = 10) (NL 60 years, n = 10) (NL < 60 years, n = 11)	↓ (741 ± 306) [*] ↓ (1022 ± 331) [*] (1523 ± 294) (1529 ± 341)	No difference (5746–6599) (5425–6044) (5168–6062) (5217–6348)		
Erdélyi et al. (2007) ⁵ / HRTII-RCM	(A, n = 10) (D, n = 8) (L, n = 8) (NL, n = 10)	↓ (843 ± 198) [*] ↓ (920 ± 89) [*] ↓ (1,002 ± 196) [*] ↓ (1,212 ± 242)	↑ (9,131 ± 1,701) ↑ (9,775 ± 823) [*] ↑ (10,610 ± 1,059) [*] (9,858 ± 99)	↓ (523 ± 36) (544 ± 37) ↓ (476 ± 45) (544 ± 25)	Hyper-reflectivity of the peripheral stroma.
Villani et al. (2007) ⁶ /Confoscan-2	(SS, n = 35) (NL, n = 20)	↓ (985.05 ± 107.57) [*] (1485 ± 133.74)	↑ (6197.37 ± 180.34) [*] (5861.65 ± 260.40)	↓ (514.75 ± 17.14) (559.23 ± 24.46)	
Zhang et al. (2011) ⁷ /HRTII-RCM	(MDE, n = 20) (MSDE, n = 20) (NL, n = 20)	↓ (890 ± 197) [*] ↓ (746 ± 125) [*] (1228 ± 248)	↓ (9234 ± 1365) [*] ↓ (8634 ± 998) [*] (11307 ± 1876)		

TSCM: Tandem scanning confocal (model 165A); **HRT-RCM:** Heidelberg Retina Tomograph-Rostock Cornea Module; **NL:** Normal; **SS:** Sjögren's Syndrome; **SSI:** Primary Sjögren's Syndrome; **NSS:** Non-Sjögren's Syndrome; **A:** Aqueous tear deficiency; **D:** Dysthyroid ophthalmopathy; **L:** Chronic Lagophthalmos; **MDE:** Mild Dry Eye; **MSDE:** Moderate to Severe Dry Eye; ↓: Increased compared to normal controls; ↓: Decreased compared to normal controls.

^{*} (P < 0.05)

TABLE 2

Corneal nerves changes by IVCN in dry eye-related conditions.

Study/ Machine	Dry Eye conditions, Patient No.	IVCM nerve changes in dry eye vs. normal controls		
		Sub-basal density	Stromal density ($\mu\text{m}/\text{mm}^2$)	Morphology
Benitez del Castillo et al. (2007) ¹¹ / Confoscan-4	(SSI, n = 10) (NSS, n = 11) (NL 60 years, n = 10) (NL < 60 years, n = 10)	↓ Total length of nerve fibers (μm) within an area of 74,340 (μm^2) ↓ (511 ± 106) [*] ↓ (591 ± 90) [*] (620 ± 92) (787 ± 105)	-----	↑ Tortuosity; ↑ Beading
Tuominen et al. (2003) ³ /TSCM	(SS, n = 10) (NL, n = 10)	No Difference	-----	↓ Nerves diameter
Villani et al. (2007) ⁶ /Confoscan-2	(SS, n = 35) (NL, n = 20)	↓ Nerves no./frame (the frame size is not mentioned in the reference) ↓ (3.34 ± 0.76) [*] (5.10 ± 0.79)	-----	↑ Tortuosity; Hyper-reflectivity
Tuisku et al. (2008) ¹² /Confoscan-3	(SSI, n = 20) (NL, n = 10)	No difference in Nerves no./0.136 mm ² (5.9 ± 2.2) (6.1 ± 2.5)	-----	↑ Stromal nerves diameter in SSI
Ho al et al. (2005) ¹³ /Confoscan-2	(SSI, n = 10) (NSS, n = 6) (NL, n = 10)	No difference	No difference	↑ Sub-epithelial nerves diameter in SSI
Zhang et al. (2005) ¹⁴ /Confoscan-2	(SSI, n = 8) (NSS, n = 30) (NL, n = 30)	↑ (1745.4 ± 414.7) [*] (1423.5 ± 609.5) (1315.7 ± 664.7) Results were reported as the total length of nerves (μm)/ frame (the frame size is not mentioned in the reference)		↑ Tortuosity; ↑ Beading; ↑ Branching
Zhang et al. (2011) ⁷ /HRTII-RCM	(MDE, n = 20) (MSDE, n = 20) (NL, n = 20)	-----	-----	↑ Tortuosity
Calvillo et al. (2004) ³⁰ /TSCM	(2–3 years after surgery)/ (LASIK, n = 11) (NL, n = 11)	↓ (3169) [*] ($\mu\text{m}/\text{mm}^2$) (6188) ($\mu\text{m}/\text{mm}^2$)	↓ (3351) [*] ($\mu\text{m}/\text{mm}^2$) (9731) ($\mu\text{m}/\text{mm}^2$)	– Recovery period starts after 6 months. – 60% of the preoperative nerves remain after 3 years.
Erie et al. (2005) ²⁹ /TSCM	(5 years after surgery) (PRK, n = 11) (LASIK, n = 12) (NL < 60 years, n = 11) (NL > 60 years, n = 12)	-----	-----	Nerve regeneration appears to remain incomplete. – 1 year after PRK: ↓ sub-basal density (59 %) – 2 years after PRK: sub-basal remain steady – 5 years after PRK: reaching density less than preoperative status. – 1 years after LASIK: ↓ sub-basal density (51%) – 2 years after LASIK: ↓ sub-basal density (35%) – 5 years after LASIK: recovery (24%)
Malik et al. (2003) ³³ /Confoscan-4	(MiDM, n = 4) (MoDM, n = 7) (SeDM, n = 7) (NL, n = 18)	↓ ($10.8 \pm 0.9\text{mm}/\text{mm}^2$) [*] ↓ ($7.5 \pm 1.1\text{mm}/\text{mm}^2$) [*] ↓ ($4.3 \pm 1.5\text{mm}/\text{mm}^2$) [*]	-----	

Study/ Machine	Dry Eye conditions, Patient No.	IVCM nerve changes in dry eye vs. normal controls		
		Sub-basal density	Stromal density ($\mu\text{m}/\text{mm}^2$)	Morphology
		($13.5 \pm 0.3\text{mm}/\text{mm}^2$)		
Kallinikos et al. (2004) ³² / Confoscan-4	(MiDM, n = 4) (MoDM, n = 7) (SeDM, n = 7) (NL, n = 18)	-----	-----	↑ Tortuosity
Rosenberg et al. (2000) ³⁴ /TSCM	Diabetes (No-Neuro, n = 11) (Mild-Moderate- Neuro, n = 7) (Severe Neuro, n = 5) (NL, n = 9)	↓ (4.0 ± 1.2) nerves per image ↓ (2.6 ± 1.4) * nerves per image ↓ (1.8 ± 0.8) * nerves per image (4.9 ± 1.1) nerves per image	-----	-----
Hamrah et al. (2010) ²⁷ /Confoscan-4	(NK-HSV, n = 31) (NL, n = 15)	↓ (448.9 ± 409.3) * (2258.4 ± 989) (Results were reported as nerve length (μm) / frame (0.158mm^2))	-----	No difference in tortuosity
Cruzat et al. (2011) ¹⁶ /HRT3-RCM	(BK, n = 23) (FK, n = 13) (AK, n = 17) (NL, n = 20)	↓ ($824.0 \pm 1,050.7$) * ↓ ($956.9 \pm 1,093.0$) * ↓ (215.6 ± 575.4) * ($3,913.9 \pm 507.4$) (Results were reported as nerve length (μm) / frame (0.16mm^2))	-----	-----

TSCM: Tandem scanning confocal (model 165A); **HRT-RCM:** Heidelberg Retina Tomograph-Rostock Cornea Module; **NL:** Normal; **SS:** Sjögren's Syndrome; **SSI:** Primary Sjögren's Syndrome; **NSS:** Non-Sjögren's Syndrome; **MDE:** Mild Dry Eye; **MSDE:** Moderate to Severe Dry Eye; **LASIK:** Laser-Assisted in Situ Keratomileusis; **PRK:** Photo-Refractive Keratectomy; **MiDM:** Mild Diabetes; **MoDM:** Moderate Diabetes; **SeDM:** Severe Diabetes; **Neuro:** Neuropathy; **NK-HSV:** Neurotrophic Keratopathy in Herpes Simplex Keratitis; **BK:** Bacterial Keratitis; **FK:** Fungal Keratitis; **AK:** *Acanthamoeba* Keratitis. ↑: Increased compared to normal controls, ↓: Decreased compared to normal controls.

*
($P < 0.05$).

TABLE 3

Corneal immune and inflammatory cell changes by IVCN in dry eye-related conditions.

Study/ Machine	Dry Eye conditions, Patient No.	IVCM inflammatory cells changes in dry eye vs. normal controls		
		Peripheral density (cells/mm ²)	Central density (cells/mm ²)	Morphology
Lin et al. (2010) ¹⁷ /HRT3- RCM	(SS, n = 14) (NSS, n = 32) (NL, n = 33)	Dendritic Cells (DCs)	Dendritic Cells (DCs)	↑ Dendrites of DCs in the central cornea
		↑↑ (157.2 ± 29.7)*	↑↑ (127.9 ± 23.7)*	
		↑ (106.9 ± 10.5)* (90.7 ± 8.2)	↑ (89.8 ± 10.8)* (34.9 ± 5.7)	
		No significant difference of DCs with processes	Dendrites of DCs	
		Non-dendritic leukocytes	↑↑ (46.1 ± 17.3)*	
		↑↑ (84.2 ± 36.8)* (8.4 ± 3.1)	↑ (9.9 ± 1.7)* (3.2 ± 0.5)	
		(4.3 ± 1.3)	Non-dendritic leukocytes	
			↑↑ (49 ± 12.9)* ↑ (4.6 ± 1.0)* (1.6 ± 0.6)	
Cruzat et al. (2011) ¹⁶ /HRT3- RCM	(BK, n = 23) (FK, n = 13) (AK, n = 17) (NL, n = 20)	-----	↑ (441.1 ± 320.5)*	↑ Maturation of dendritic cells ↑ Size and dendrites number.
			↑ (608.9 ± 812.5)*	
			↑↑ (1000.2 ± 1090.3)* (49.3 ± 39.6)	
Tuisku et al. (2008) ¹² / Confoscan-3	(SSI, n = 20) (NL, n = 10)	-----	-----	↑ Sub-basal nerve plexus infiltration with mature Antigen Presenting Cells (APCs).

HRT-RCM: Heidelberg Retina Tomograph-Rostock Cornea Module; **NL:** Normal; **SS:** Sjögren's Syndrome; **SSI:** Primary Sjögren's Syndrome; **NSS:** Non-Sjögren's Syndrome; **BK:** Bacterial Keratitis; **FK:** Fungal Keratitis; **AK:** *Acanthamoeba* Keratitis. ↑: Increased compared to normal controls, ↓: Decreased compared to normal controls.

*
($P < 0.05$).

TABLE 4

Morphological changes of meibomian glands by IVCM in dry eye-related conditions.

IVCM meibomian glands changes in dry eye vs. normal controls						
Study/ Machine	Dry Eye conditions, Patient No.	Acinar density (unit/mm ²)	Acinar diameter (μ m)	Orifice diameter (μ m)	Meibum reflectivity (Grade 1–4)	Morphology
Villani et al. (2011) ¹⁹ / HRTII-RCM	(CLWs, n = 20) (NL, n = 20)	No difference (129 \pm 48) (119 \pm 22)	\downarrow (36 \pm 8) [*] (45 \pm 9)	\uparrow (44 \pm 16) [*] (33 \pm 7)	\uparrow (2.2 \pm 0.5) [*] (1.2 \pm 0.4)	\downarrow Basal epithelial cell density.
Villani et al. (2011) ¹⁸ / HRTII-RCM	(SSI, n = 20) (SSII, n = 25) (MGD, n = 20) (NL, n = 20)	\uparrow (138 \pm 69) \uparrow (97 \pm 43) \uparrow (57 \pm 21) (110 \pm 31)	(53 \pm 31) \uparrow (70 \pm 42) \uparrow (106 \pm 41) (53 \pm 14)	\downarrow (27.8 \pm 5.9) [*] \downarrow (20.6 \pm 5.1) [*] \uparrow (50 \pm 9.1) [*] (34.7 \pm 4.3)	\uparrow (1.7 \pm 0.6) [*] \uparrow (2.2 \pm 0.8) [*] \uparrow (3.3 \pm 0.7) [*] (1.1 \pm 0.7)	\uparrow Periglandular inflammation. \uparrow Basal epithelium cell density was significantly. \downarrow No differences in superficial epithelium cell density.
Matsumoto et al. (2008) ²⁰ /HRTII-RCM	(MGD, n = 20) (NL, n = 15)	\downarrow (47.6 \pm 26.6) [*] (101.3 \pm 33.8)	\uparrow (98.2 \pm 53.3) [*] (41.6 \pm 11.9)	-----	-----	\uparrow Glandular acinar units. \downarrow Hyperkeratinization of ductal epithelium.
Ibrahim et al. (2010) ²¹ / HRTII-RCM	(MGD, n = 20) (NL, n = 26)	\downarrow (67.8 \pm 15.1) [*] (113.7 \pm 36.6)	Longest diameter \uparrow (86.3 \pm 18.9) [*] (56.3 \pm 10.4) Shortest diameter \uparrow (34.8 \pm 9.2) [*] (17.4 \pm 4.2)	-----	-----	\uparrow Infiltration and enlargement of glandular acinar units. \uparrow Periglandular inflammatory cell (1026.1 \pm 537.3 compared to normal 56.6 \pm 32.1 cells/mm ²)
Matsumoto et al. (2009) ³⁶ /HRTII-RCM	(OMGD+/ Anti-Inflammation, n = 16) (OMGD/No Anti-Inflammation, n = 11)	-----	-----	-----	\uparrow A (2.4 \pm 0.6) B (2.3 \pm 0.5) A (2.0 \pm 0.5) B (2.0 \pm 0.5)	\downarrow Inflammatory cells density (cells/mm ²) \downarrow (700 \pm 436) [*] (1216 \pm 328) \downarrow (843 \pm 321) (882 \pm 301)

HRT-RCM: Heidelberg Retina Tomograph-Rostock Cornea Module; **NL:** Normal; **CLWs:** Contact lens wearers; **SSI:** Primary Sjögren's Syndrome; **SSII:** Secondary Sjögren's Syndrome; **MGD:** Meibomian Gland Dysfunction; **OMGD:** Obstructive Meibomian Gland Disease; \uparrow : Increased compared to normal controls; \downarrow : Decreased compared to normal controls.

^{*} (P < 0.05),

A: After treatment; B: Before treatment.

TABLE 5

Conjunctival changes by IVCN in dry eye-related conditions.

Study/ Machine	Dry Eye conditions, Patient No.	IVCM conjunctiva changes in dry eye vs. normal controls		
		Presumed Epithelial cell density (cells/mm ²)	Presumed Goblet cell density (cells/mm ²)	Morphology
Wakamatsu et al. (2010) ²⁴ /HRTII-RCM	(SS, n = 28) (NSS, n = 7) (NL, n = 14)	-----	-----	– ↑ Density of epithelial cysts in SS. – ↑ Inflammatory cells density: ↑ (433 ± 435.8) * ↑ (134.8 ± 124.2) * (10 ± 17.9)
Hong et al. (2010) ²² / HRT3-RCM vs. IC	(SS, n = 43)	-----	IVCM (332 ± 137) IC (200 ± 141)	Significant positive correlation between IVCM and IC Goblet Cell densities
Villani et al. (2011) ²³ / HRTII-RCM	(SS, n = 24) (NLY, n = 12) (NLO, n = 12)	↑ (4331 ± 1114) * (2515 ± 303) (1819 ± 502)	↑ (688 ± 318) * (36 ± 41) (325 ± 431)	↑ Inflammatory cells density ↑ (1662 ± 818) * (717 ± 390) (905 ± 382)

HRT-RCM: Heidelberg Retina Tomograph-Rostock Cornea Module; **IC:** Impression Cytology; **NLY:** Normal Young ~24 years; **NLO:** Normal Old ~68 years; **SS:** Sjögren's Syndrome; **NSS:** Non-Sjögren's Syndrome. ↑: Increased compared to normal controls, ↓: Decreased compared to normal controls.

* (P < 0.05).